Magnetic force microscopy of vortex pinning at grain boundaries in superconducting thin films

A. Volodin [a,*], K. Temst [a], Y. Bruynseraede [a], C. Van Haesendonck [a],
M.I. Montero [b], Ivan K. Schuller [b], B. Dam [c], J.M. Huijbregtse [c], R. Griessen [c]

[a] *Laboratorium voor Vaste-Stoffysica en Magnetisme, Katholieke Universiteit Leuven, Celestijnenlaan 200 D, B-3001 Leuven, Belgium*
[b] *Department of Physics, University of California-San Diego, La Jolla, CA 92093-0319, USA*
[c] *Faculty of Sciences, Division of Physics and Astronomy, Vrije Universiteit, De Boelelaan 1081,
NL-1081 HV Amsterdam, The Netherlands*

Abstract

We succeeded to image with magnetic force microscopy individual vortices in thin Nb films as well as in thin $YBa_2Cu_3O_{7-\delta}$ (YBCO) films. Relying on the imaging of microfabricated gold loops, we are able to identify the exact location of the vortices within 10 nm with respect to topographic features. The center of most of the vortices is located in between the grains appearing at the film surface. For the Nb films with a larger coherence length, the pinning can be linked to the reduced film thickness in between the protruding grains. For the YBCO films with a very small coherence length, the pinning is likely to be dominated by line defects at the trenches in between the growth islands. On the other hand, Fourier analysis of the imaged vortex distribution shows that for thicker Nb films not all of the vortices are pinned in between the grains. Due to the vortex–vortex repulsion, the vortex lattice reveals short-range correlations which become more pronounced at higher fields. © 2001 Elsevier Science B.V. All rights reserved.

PACS: 74.60.Ge; 68.37.RT
Keywords: Flux pinning; Magnetic force microscopy

1. Introduction

The discovery of high-T_c superconductivity has resulted in a revival of the interest to prepare materials with very high superconducting current densities in the presence of a magnetic field. The direct link between the critical current density and the presence of specific defect structures continues to attract a lot of attention [1].

The direct imaging of individual vortices in the mixed state of a superconductor is one of the most challenging applications of magnetic force microscopy (MFM) [2]. An important advantage of MFM is the possibility to measure the magnetic stray field induced by the vortices and the sample topography at the same location. The MFM imaging allows to correlate the pinning of vortices with the presence of specific defects such as grain boundaries and other extended lattice defects.

---

* Corresponding author.
E-mail address: alexander.volodin@fys.kuleuven.ac.be (A. Volodin).

Here, we present the results we obtained with low-temperature MFM on superconducting thin Nb films as well as on thin films of the YBCO high-T_c superconductor. We are able to establish a direct link between the position of the vortices and the presence of topographical features related to the film growth. Moreover, for the Nb films our MFM images allow to visualize the gradual ordering which occurs in the vortex distribution when increasing the Nb film thickness [3].

2. Experiment

The thin Nb films have been deposited by electron beam evaporation in an ultrahigh vacuum molecular beam epitaxy (MBE) system with a base pressure around 10^{-8} Pa. The deposition of the thin films onto oxidized Si (1 0 0) wafers is performed at room temperature at a rate of about 0.01 nm/s [4]. The film thickness is determined by low angle X-ray scattering. The high-angle diffraction spectra confirm that the Nb thin films are polycrystalline with a preferred growth along the (1 1 0) direction, but with a random distribution of the in-plane grain orientation. Electrical transport measurements reveal an increase of the transition temperature T_c from 7.5 K towards the bulk value 9.2 K when increasing the Nb film thickness t from 25 to 100 nm (see Table 1). Both the transition width ($\leqslant 0.1$ K) and the normal state resistivity at 10 K (10–15 $\mu\Omega$ cm) confirm the quality of the MBE grown Nb films. Thin films of $YBa_2Cu_3O_{7-\delta}$ (YBCO) were deposited on (1 0 0) $SrTiO_3$ substrates by means of pulsed laser deposition (PLD). Our PLD set-up consists of a KrF excimer laser, beam projection optics, and a high vacuum system with a base pressure of 10^{-4} Pa. The optical components ensure a spatially homogeneous laser spot

on the target, which is essential to achieve a stoichiometric film. The 140-nm-thick films are ablated from a rotating, polycrystalline, high density, stoichiometric, tetragonal $YBa_2Cu_3O_{6+x}$ target at an oxygen background pressure of 15 Pa, at a substrate temperature of 815 °C. The laser energy density is fixed at 1.4 J/cm^2. The films are epitaxially oriented with the c-axis normal to the substrate surface [5]. The films reveal concentric growth steps, showing that they grow by two-dimensional (2D) nucleation and growth. In PLD, spiral growth is only observed under special growth conditions [6]. Screw dislocations are therefore not expected to be found at the center of these growth islands. Indeed, using wet chemical etching, we demonstrated that in our PLD films dislocations, both of screw and edge type, are only found in the trenches between the 2D-growth islands [1,7].

Our low temperature MFM is based on cantilevers integrated with piezoresistive displacement detection [8,9]. The sensing element is a piezoresistor embedded in the arms of the cantilever [10]. The resistance change of the piezoresistor caused by stresses due to cantilever deflection can easily be measured. The fundamental resonance frequency is in the range 30–50 kHz, while the force constant is about 1 N/m. Such cantilevers are ideally suited for operation at low temperatures, because they do not require optical detection of the cantilever deflection with a complicated in situ adjustment of the optical beam. MBE deposition is used to grow on top of the Si tips two 25-nm-thick Co layers separated by a 2-nm-thick Au layer. Oblique incidence deposition minimizes the coated area by restricting the magnetic film growth to one side of the tip in order to decrease the influence of the MFM tip fringe field on weakly pinned vortices.

All measurements reported in this paper have been performed under field cooled conditions. Our MFM is able to resolve individual vortices when cooling the films below T_c in relatively low magnetic fields (<10 mT) [9]. This is confirmed by the fact that the density of vortices observed with our MFM corresponds to the ratio between the applied magnetic field and the superconducting flux quantum $\Phi_0 = h/2e = 2.07 \times 10^{-15}$ Wb = 2.07 mT/μm^2. An

Table 1
Relevant parameters of the Nb films and the YBCO film

Sample	Nb1	Nb2	Nb3	YBCO
Thickness (nm)	32	33	87	140
RMS roughness (nm)	1.4	1.4	2	6
Grain size (nm)	24	27	32	210
Critical temperature (K)	7.9	8.4	9.1	91

increase of the field above 10 mT leads to an almost complete loss of the MFM contrast due to the overlap between the magnetic fields of neighboring vortices.

In order to image the vortices, the following procedure is used [11]. The tip is first brought into contact with the sample surface at a temperature above T_c in the normal state. The (x, y) scan plane is then adjusted to coincide with the investigated surface. Next, the tip is raised above the surface towards a height exceeding 1 μm. After cooling down to 4.3 K in a magnetic field perpendicular to the film surface, the tip-to-sample separation is decreased to a fixed separation, ranging between 20 and 50 nm. Finally, while scanning the tip across the (x, y) plane, we record the phase shift of the oscillation of the cantilever due to the magnetic interaction between sample and tip.

The possible influence of the magnetic stray field produced by the tip on the superconducting surface has been checked in detail for the Nb films. Measurements taken at different magnetic fields point towards the existence of an offset field $B_{\text{tip}} = 0.3–0.5$ mT at zero applied field, which corresponds to the extra field induced by our MFM tips [11,12]. The field B_{tip} is sufficiently small to be able to perform reliable non-invasive imaging of the vortex distribution.

In order to measure the surface topography, the tip-to-sample distance is decreased to allow operation of the MFM in the near-field, non-contact atomic force microscopy (AFM) regime, providing a pure topographic contrast. The topographic image is acquired at the same position as the magnetic image. Below, we will describe in detail how we are able to correlate with a high spatial resolution the location of the vortices with specific topographic features appearing on the Nb and YBCO film surfaces.

3. Experimental results

Fig. 1(a) shows a typical example of an unfiltered MFM image of the vortex distribution at 4.3 K under field cooled conditions at 4 mT for the thin film sample Nb2 (see Table 1). The corresponding topographic AFM image is shown in
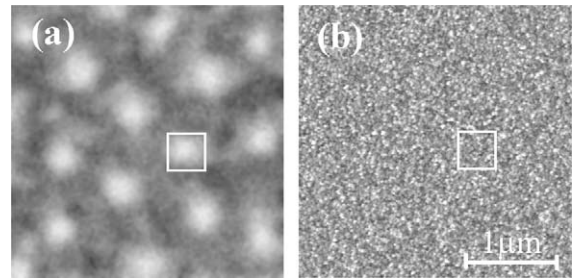

Fig. 1. (a) Unfiltered MFM image (3×3 μm^2) for the Nb film Nb2 (see Table 1) cooled in a field of 4 mT. (b) Surface topography acquired at the same location (the grey scale contrast corresponds to height variations of 8 nm).
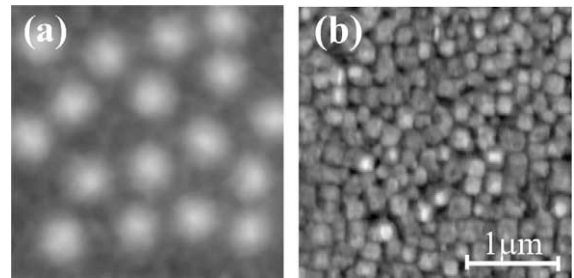

Fig. 2. (a) Low-pass filtered MFM image (3×3 μm^2) for the YBCO film (see Table 1) cooled in an external field of 4 mT. (b) Surface topography acquired at the same location (the grey scale contrast corresponds to height variations of 20 nm).

Fig. 1(b). Fig. 2(a) shows a low-pass filtered MFM image of the vortex distribution at 4.3 K under the same field cooled conditions for the high-T_c YBCO thin film (see Table 1). In Fig. 2(b) we give the corresponding topographic AFM image. Both the YBCO and Nb surfaces reveal a typical texture with different grain sizes. The grains in the Nb films have an ellipsoidal shape [13], while the YBCO film is composed of growth islands separated by more pronounced trenches [1].

In order to determine the exact location of the vortices with respect to features appearing in the topographic AFM image, it is necessary to take into account the asymmetry of the magnetic charge distribution about the tip apex [14]. The asymmetry shifts the magnetic image with respect to the topographic image. In order to determine this shift, Hug et al. [14] suggested to rely on a transfer function approach. The transfer function of the tip

can be inferred from the geometrical shape of the tip. We used an alternative approach which is based on MFM imaging of a microfabricated gold loop [15]. The MFM image and the topographic image are recorded while feeding a current of several mA through the loop. The shift of the MFM image is calculated by comparing the co-ordinates of the centers of the MFM image and the topographic image, respectively. Calculated values of the shift for different tips range between 10 and 40 nm.

The location of the vortices on the MFM images is determined by fitting a Gaussian profile to their MFM signal after low-pass filtering (see upper panels in Fig. 3(c) and (f)). Taking into account the calculated shift of the MFM image with respect to the topographic image, we are able to obtain the exact location of the magnetic vortices with respect to the surface topography shown in Fig. 3(b) and (e). The accuracy of this procedure is better than 10 nm, indicating that we are able to distinguish between on-grain and inter-grain flux pinning. We note that the validity of our correction procedure is supported by MFM images taken at smaller tip-to-sample distances, where the film topography contributes to the MFM image contrast (see Fig. 3(a) and (d)). Similar to Ref. [16], the topographical contribution can be recognized as white spots with a size below our MFM resolution (~100 nm). The typical grain sizes of our Nb films and of our YBCO film are 30 and 200 nm, respectively (see Table 1). We note that even for our Nb films the diameter of the normal core of a vortex $2\xi \approx 22$ nm [4] (ξ is the superconducting coherence length) remains smaller than the typical grain size.

Combining for each of the Nb films and for the YBCO film (see Table 1) the results of the MFM measurements in an external field of 2.5 mT with the corresponding topographic images, we find that a larger fraction of the vortex pinning occurs in between the grains. This is illustrated by the chart shown in Fig. 4 which gives the percentage fraction for the two possible vortex locations (on-grain and inter-grain).

According to Fig. 4 all vortices in the YBCO film are pinned at locations in between the growth islands of the pulsed laser deposited films. These
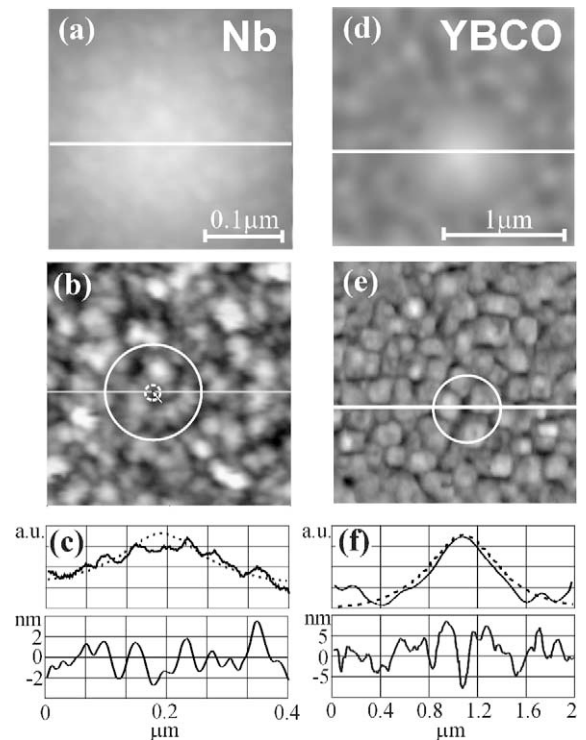

Fig. 3. (a) Enlarged MFM image (0.3×0.3 μm², see white squares in Fig. 1) for the Nb film Nb2 and (b) the corresponding topographic image. (d) MFM image of a single vortex (2×2 μm²) in the YBCO film and (e) the corresponding topographic image. The white circles in (b) and (e) correspond to the distance at which the stray field emanating from the vortex has decreased to $1/e$ of its maximum value. The small dotted circle in (b) defines an area with diameter $2\xi \approx 22$ nm [14] (ξ is the superconducting coherence length). The lower panels (c) and (f) are cross-sections of the MFM data and the topography profiles along the white lines indicated in (a), (b), (d) and (e). The dotted curves correspond to a Gaussian profile fitting the MFM signal after filtering with a low-pass filter.

pinning centers are likely to correspond to the linear defects, which have been observed to end at the trenches in between the growth islands [1]. Although e.g. grain boundary pinning has been suggested [17], no direct correlation with such boundaries could be made.

The chart in Fig. 4 further reveals that for the Nb films the preferential pinning at locations in between grains becomes more pronounced for the thinner films (films with lower T_c). Obviously, the pinning mechanism in the Nb films is different
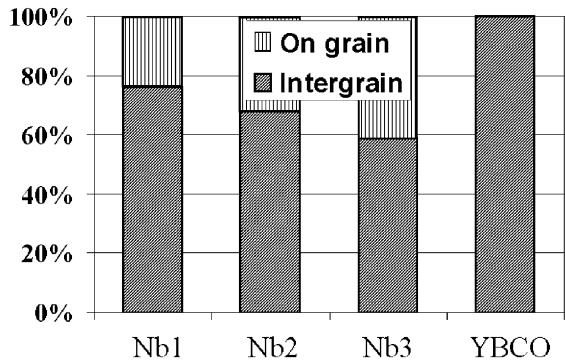
Fig. 4. Chart illustrating the preferential location of the vortices in between the grains of the YBCO film and of the Nb films with different thickness, i.e., with different critical temperature T_c (see Table 1).

Fig. 5. Filtered MFM images ($6 \times 6 \ \mu m^2$) of the vortex arrangement (a,c) and the corresponding 2D Fourier transforms (b,d) for the Nb films Nb1 and Nb3 (see Table 1) with different thickness. The films have been cooled in the presence of a magnetic field of 4 mT.

from that in YBCO. Instead of the 2–3 nm coherence length ξ_{ab} in YBCO, which is of the same order of magnitude as the core of dislocation, in Nb the coherence length is about 11 nm. This is comparable to the width of the depressions between the grains. Since the grains are well-connected electrically, pinning is likely to occur between the protruding Nb grains, because of the considerable local reduction of the film thickness. From the topographical cross-section in the lower panel of Fig. 3(c) we infer a thickness reduction of about 4 nm or 1/8 of the film thickness, which should be sufficient to induce pinning. In the thicker Nb films with a higher T_c less vortices are pinned in between grains. This is consistent with the vortex–vortex interaction becoming more dominant when compared to the pinning strength.

The tendency to form a more regular vortex lattice in the thicker Nb films [3] is illustrated in more detail in Fig. 5, where we present the measured distribution of the vortices for two different Nb film thicknesses together with the corresponding 2D Fourier transform of the MFM images. The Fourier transform of the thicker Nb film clearly reveals the six discrete spots which are expected for the triangular Abrikosov vortex lattice with hexagonal symmetry. The appearance of the hexagonal lattice confirms that the arrangement of vortices is no longer dominated by pinning alone, but also by the vortex–vortex interaction which induces short-range order in the vortex distribu-
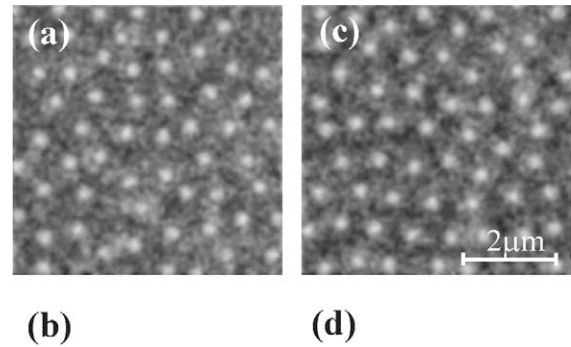
tion. A gradual ordering of the vortex lattice is also observed in Nb films when increasing the applied magnetic field. This is illustrated in Fig. 6,
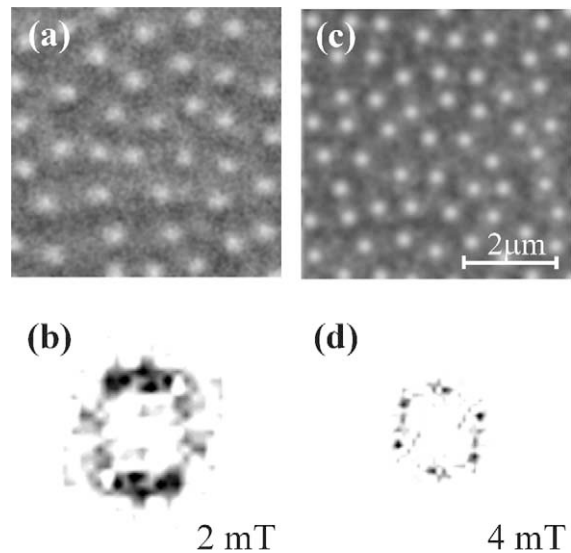

Fig. 6. Filtered MFM images ($6 \times 6 \ \mu m^2$) of the vortex arrangement and the corresponding 2D Fourier transforms for the Nb film Nb3 (see Table 1) for different applied magnetic fields: (a) 2 mT and (c) 4 mT.

where both the MFM image and the corresponding 2D Fourier transform are shown at two different fields for the Nb film Nb3. On the other hand, we do not observe any indication of short-range order in the vortex arrangement for the YBCO film in the range 0.5–2.5 mT.

4. Conclusions

We demonstrated the possibility to reliably measure with a low-temperature MFM the magnetic stray field of vortices in thin films of both the conventional superconductor Nb and the high-T_c superconductor YBCO. Moreover, our force microscope enables to monitor the surface topography at the same location. This allows to correlate the pinning of the vortices for fields below 10 mT with specific topographic features. We find that the vortex pinning preferentially occurs in between the grains composing the films. For the Nb films we find that preferential inter-grain pinning becomes more pronounced in thinner films and when increasing the applied magnetic field. In YBCO films, all of the imaged vortices are pinned in between the growth islands. Our results are consistent with previous observations of vortices in similar YBCO films [16], and agree with the fact that the superconducting current density is field independent below the so-called characteristic magnetic field B^* [7], which is typically 10–100 mT. The size of this characteristic field could be correlated with the density of strongly pinning dislocations [1]. In fact $B^* \sim B_\Phi = n_{disl}\Phi_0$ (n_{disl} is the dislocation density). Since the applied field for our MFM measurements does not exceed 2.5 mT, i.e., remains considerably smaller than the typical characteristic fields, a strong pinning dislocation is available for all vortices, explaining the lack of vortex ordering in YBCO at sufficiently small magnetic fields [1].

References

[1] B. Dam, J.M. Huijbregtse, F.C. Klaassen, R.C.F. van der Geest, G. Doornbos, J.H. Rector, A.M. Testa, S. Freisem, J.C. Martinez, B. Stäuble-Pümpin, R. Griessen, Nature 399 (1999) 439;
F.C. Klaassen, G. Doornbos, J.M. Huijbregtse, R.C.F. van der Geest, B. Dam, R. Griessen, Phys. Rev. B 64 (2001) 184523.

[2] A. Moser, H.J. Hug, I. Parashikov, B. Sfiefel, O. Fritz, H. Thomas, A. Baratoff, H.-J. Güntherodt, Phys. Rev. Lett. 74 (1995) 1847.

[3] A. Volodin, K. Temst, C. Van Haesendonck, Y. Bruynseraede, M.I. Montero, Ivan K. Schuller, Europhys. Lett., submitted for publication.

[4] A. Hoffmann, Doctoral Thesis, University of California, San Diego, 1999.

[5] J.M. Huijbregtse, B. Dam, J.H. Rector, R. Griessen, J. Appl. Phys. 86 (1999) 6528.

[6] B. Dam, J.H. Rector, J.M. Huijbregtse, R. Griessen, Physica C 305 (1998) 1.

[7] J.M. Huijbregtse, B. Dam, R.C.F. van der Geest, F.C. Klaassen, R. Elberse, J.H. Rector, R. Griessen, Phys. Rev. B 62 (2000) 1338.

[8] C.W. Yuan, E. Batalla, M. Zacher, A.L. De Lozanne, M.D. Kirk, M. Tortonese, Appl. Phys. Lett. 65 (1994) 1308.

[9] A. Volodin, K. Temst, C. Van Haesendonck, Y. Bruynseraede, Appl. Phys. Lett. 73 (1998) 1134.

[10] TM Microscopes, Veeco Metrology Group, 1171 Borregas Avenue Sunnyvale, CA 94089, USA.

[11] A. Volodin, K. Temst, C. Van Haesendonck, Y. Bruynseraede, Rev. Sci. Instrum. 71 (2000) 4468.

[12] A. Volodin, K. Temst, C. Van Haesendonck, Y. Bruynseraede, Physica C 332 (2000) 156.

[13] Y. Tarutani, M. Hirano, U. Kawabe, Proc. IEEE 27 (1989) 1164.

[14] H.J. Hug, B. Stiefel, P.J.A. van Schendel, A. Moser, R. Hofer, S. Martin, H.-J. Güntherodt, J. Appl. Phys. 83 (1998) 5609.

[15] Kong Linshu, S.Y. Chou, Appl. Phys. Lett. 70 (1997) 2043.

[16] H.J. Hug, P.J.A. van Schendel, B. Stiefel, O. Knauff, Ch. Loppacher, S. Martin, H.-J. Güntherodt, J.M. Huijbregtse, B. Dam, R. Griessen (unpublished).

[17] E. Mezzetti, R. Gerbaldo, G. Ghigo, L. Gozzelino, B. Minetti, C. Camerlingo, A. Monaco, G. Cuttone, A. Rovelli, Phys. Rev. B 60 (1999) 7623.